Applied and Environmental Microbiology, Oct. 2007, p. 6150–6158 Vol. 73, No. 19
0099-2240/07/$08.00+0 doi:10.1128/AEM.02830-06

Phototrophic Fe(II) Oxidation Promotes Organic Carbon Acquisition by *Rhodobacter capsulatus* SB1003▽

Nicky C. Caiazza,[1,3] Douglas P. Lies,[1,3] and Dianne K. Newman[1,2,3]*

Division of Geological and Planetary Sciences,[1] Division of Biology,[2] and Howard Hughes Medical Institute,[3] California Institute of Technology, Pasadena, California 91125

Received 5 December 2006/Accepted 1 August 2007

Anoxygenic phototrophic Fe(II) oxidation is usually considered to be a lithoautotrophic metabolism that contributes to primary production in Fe-based ecosystems. In this study, we employed *Rhodobacter capsulatus* SB1003 as a model organism to test the hypothesis that phototrophic Fe(II) oxidation can be coupled to organic carbon acquisition. *R. capsulatus* SB1003 oxidized Fe(II) under anoxic conditions in a light-dependent manner, but it failed to grow lithoautotrophically on soluble Fe(II). When the strain was provided with Fe(II)-citrate, however, growth was observed that was dependent upon microbially catalyzed Fe(II) oxidation, resulting in the formation of Fe(III)-citrate. Subsequent photochemical breakdown of Fe(III)-citrate yielded acetoacetic acid that supported growth in the light but not the dark. The deletion of genes (RRC00247 and RRC00248) that encode homologs of *atoA* and *atoD*, required for acetoacetic acid utilization, severely impaired the ability of *R. capsulatus* SB1003 to grow on Fe(II)-citrate. The growth yield achieved by *R. capsulatus* SB1003 in the presence of citrate cannot be explained by lithoautotrophic growth on Fe(II) enabled by indirect effects of the ligand [such as altering the thermodynamics of Fe(II) oxidation or preventing cell encrustation]. Together, these results demonstrate that *R. capsulatus* SB1003 grows photoheterotrophically on Fe(II)-citrate. Nitrilotriacetic acid also supported light-dependent growth on Fe(II), suggesting that Fe(II) oxidation may be a general mechanism whereby some Fe(II)-oxidizing bacteria mine otherwise inaccessible organic carbon sources.

The discovery of anoxygenic phototrophic Fe(II)-oxidizing bacteria was first reported in the 1990s (14, 21, 43), nearly 20 years after Garrels and Perry postulated that these organisms could have been dominant players in ancient Fe-based aquatic ecosystems (17). The photosynthetic reaction center of these organisms uses light energy and electrons from Fe(II) to generate cellular energy in the form of ATP and reducing equivalents in the form of NAD(P)H. The latter is used to convert CO_2 into biomass; thus, Fe(II) oxidization can be used to support photoautotrophic growth. Fe(II)-oxidizing phototrophs do not always couple Fe(II) oxidation to autotrophic growth; however, some strains oxidize Fe(II) while growing photoheterotrophically on an organic substrate, such as acetate or succinate (14, 22). In these cases, it is not clear whether Fe(II) oxidation benefits the cell.

Recently, phototrophic Fe(II) oxidation has gained attention for the potential role it might have played in the deposition of Archaean and early Proterozoic banded iron formations (14, 20, 26, 43). This metabolism is also interesting from the perspective of the evolution of photosynthesis. Of all reductants known to support anoxygenic photosynthesis, ferrous iron [Fe(II)] has the highest midpoint potential and may have been a transitional electron donor during the evolution of H_2O-accommodating reaction centers (31–33).

Interestingly, one aspect often neglected in studies or models pertaining to biologically catalyzed Fe(II) oxidation is that Fe often exists in chelated forms. In organic-rich freshwater systems and the surface waters of the oceans, the vast majority of the dissolved Fe pool is strongly bound to organic ligands (18, 27, 34, 44). The presence of chelators can affect Fe(II) oxidation in multiple ways. One possibility is that the Fe(II)-chelate complex can make Fe(II) more available to the cells. This could be a factor when there is a propensity to form ferrous minerals. Another possible role for a chelator is to keep the ferric iron [Fe(III)] that is generated as a result of microbial Fe(II) oxidation in a soluble form and to prevent cell encrustation. Ferric minerals are often observed in association with the cell surfaces of cultures growing phototrophically on Fe(II) (22, 25). The chelating agent nitrilotriacetic acid (NTA) was shown to prevent the formation of crystalline precipitates on the surfaces of Fe-grown *Rhodomicrobium vannielii* cultures (22).

The presence of a chelator will also alter the thermodynamics of Fe(II) oxidation. As predicted by the Nernst equation, altering the Fe(III)/Fe(II) ratio will change the midpoint potential of the redox couple. When the midpoint potential decreases, a more reducing environment favoring Fe(II) oxidation will result. Thus, the presence of a chelator that has a higher affinity for Fe(III) than for Fe(II) can decrease the midpoint potential by preferentially depleting the pool of Fe(III) relative to Fe(II).

In addition to these effects, a frequently overlooked impact that a chelator/ligand may have on microbial Fe(II) oxidation stems from the potential photochemical reactions that can occur between the ligand and Fe(III). Such reactions have been well described in the biological oceanographic literature (4, 5, 30). For example, one class of marine siderophores contains α-carboxylate moieties, such as citrate, that are photochemically active in the presence of Fe(III). Examples include aerobactin produced by *Vibrio* sp. strain DS40M5 (28),

* Corresponding author. Present address: Department of Biology, MIT, 77 Massachussetts Ave., 68-380, Cambridge, MA 02139. Phone: (617) 324-2770. Fax: (617) 324-3972. E-mail: dkn@mit.edu.

▽ Published ahead of print on 10 August 2007.

TABLE 1. Strains, plasmids, and primers used in this study

Strain, plasmid, or primer	Properties or 5′-to-3′ primer	Reference or source
Strains		
R. capsulatus SB1003	Wild type, Rif^r	
R. capsulatus SB1003 Δ*hupSL*	Δ*hupSL*, Rif^r	This study
R. capsulatus SB1003 ΔRRC00247-RRC00248	ΔRRC00247-RRC00248, Rif^r	This study
E. coli UQ950	Cloning strain	D. Lies[b]
E. coli WM3064	Donor strain	W. Metcalf[c]
S. cerevisiae InvSC1	Ura$^-$ for gap repair cloning	Invitrogen
Plasmids		
pMQ30	Yeast-based allelic exchange vector, *sacB*,[a] CEN/ARSH, URA3$^+$, Gm^r	35
pMQ87	Yeast-based suicide vector, CEN/ARSH, URA3$^+$, Gm^r	35
pZJD29a	Allelic exchange vector, *sacB*,[a] Gm^r	C. Bauer[d]
pMQ131	Yeast-based pBBR1-based shuttle vector, CEN/ARSH, URA3$^+$, Kn^r	R. M. Q. Shanks and G. A. O'Toole[e]
pNC001	*hupSL* deletion fragments cloned into pMQ30	This study
pNC005	*hupSL* deletion fragments cloned into pZJD29a	This study
pNC006	Yeast-based allelic exchange vector, *sacB*,[a] CEN/ARSH, URA3$^+$, Gm^r	This study
pNC007	RRC00247 and RRC00248 deletion fragment cloned into pNC006	This study
pNC008	RRC00247 and RRC00248 genes clones into pMQ131, Kn^r	This study
Primers		
pnc001	GTGGAATTGTGAGCGGATAACAATTTCACACAGGA AACAGCTCTGGGCGAGAACCTTTGG	
pnc002	CCTTGACGGTGGTCAGGCAATTGTCCCTCCCTTGC	
pnc003	GCAAGGGAGGGACAATTGCCTGACCACCGTCAAGG	
pnc004	GGCAAATTCTGTTTTATCAGACCGCTTCTGCGTTCT GATCTCTTCCAGAAACGGCAGC	
pnc017	GGCGGAGCTCCTGGGCGAGAACCTTTGG	
pnc018	GGCGTCTAGACTCTTCCAGAAACGGCAGC	
pnc021	ATGCCACGATCCTCGCCCTGCTGGCGAAGATCGACT CTAGCCACAGTCGATGAATCCAG	
pnc022	ATCTCTAAGAAACCATTATTATCATGACATTAACCC GACAATTCGACCTGAAAATTCC	
pnc023	GGCAAATTCTGTTTTATCAGACCGCTTCTGCGTTCT GATGAAGATCGACGAGGTTCTGG	
pnc027	AGGTTCGAGATGATCCGGTTGAAACCCTCCCGTTAC CTTG	
pnc028	CAAGGTAACGGGAGGGTTTCAACCGGATCATCTCG AACCT	
pnc026	TGGAATTGTGAGCGGATAACAATTTCACACAGGAA ACAGCTCGAGACGGCT TTCCACAGG	
pnc033	GGCGTCTAGAATGTGAAGCACAACAGCACCTACG	
pnc034	GGCGGAGCTCATAATGGCGCAGGTTCTGCCAAAG	

[a] *sacB* in pMQ30 is under the control of the native promoter, and the *sacB* gene in pZJD29a and pNC006 is under the control of the *R. capsulatus pucAB* promoter.
[b] California Institute of Technology, Pasadena, CA.
[c] University of Illinois, Urbana, IL.
[d] University of Indiana, Bloomington, IN.
[e] Dartmouth College (www.dartmouth.edu/~gotoole/vectors.html), Hanover, NH.

ochrobactins produced by *Ochrobactrum* sp. strain SP18 (30), and synechobactins produced by *Synechococcus* PCC 7002 (24). Photochemistry between the above siderophores with Fe(III) has been documented and results in the reduction of Fe(III) and photolytic decarboxylation of the ligand (4, 5). We expect such a process to influence microbial Fe(II) oxidation in at least two ways. (i) Photochemical reactions would (re)generate Fe(II) that could then be used by organisms capable of Fe-based phototrophic metabolisms, and (ii) the photochemical breakdown of the ligand could produce organic material that could be used for heterotrophic growth.

In this study, we provide data to support the hypothesis that anoxygenic phototrophic Fe(II) oxidation can enable photoheterotrophic cell growth through the use of a ferrated-ligand that is subject to photochemical degradation. We chose citrate as a model ligand because it is a photochemically reactive moiety found in siderophores and is not used as a carbon source by many phototrophs (41). *R. capsulatus* SB1003 serves as our model organism because it does not grow photoheterotrophically on citrate or photoautotrophically on soluble Fe(II) but does oxidize Fe(II) (10). Here, we show that phototrophic Fe(II) oxidation promotes organic carbon acquisition by SB1003 and discuss the broader implications of these findings.

MATERIALS AND METHODS

Bacterial strains, media, and chemicals. All bacterial strains, plasmids, and primers used in this study are listed in Table 1. *R. capsulatus* SB1003 was grown chemoheterotrophically at 30°C in YP medium (0.3% yeast extract and 0.3% Bacto peptone [Difco]). FEM buffered at pH 6.8 with bicarbonate was used as the base medium for phototrophic growth (11, 14). For photoheterotrophic growth, FEM was supplemented with 10 mM acetate, 10 mM citrate plus 4 to 6 mM $FeCl_2$, 10 mM citrate plus 4 to 6 mM $FeCl_3$, or 10 mM NTA plus 4 to 6 mM $FeCl_2$. FEM medium containing 4 to 6 mM Fe(II) was made as described previously (11). FEM medium containing 4 to 6 mM Fe(III)-citrate was made by adding $FeCl_3$-citrate from an anoxic stock solution. The atmosphere for photoheterotrophic growth was 80% N_2:20% CO_2. For photoautotrophic growth, cells were grown in FEM with a headspace of 80% H_2:20% CO_2. Unless noted otherwise, phototrophically grown cells were incubated at 30°C under constant illumination 15 cm from a 34-W incandescent light source. *Escherichia coli* was cultured on lysogeny broth (6), and strain WM3064 was supplemented with 0.3 mM diaminopimelic acid. *Saccharomyces cerevisiae* was routinely cultured on YPD medium (1% yeast extract, 2% Bacto peptone [Difco], 2% dextrose) at 30°C or on SD medium lacking URA (Qbiogene) for gap repair cloning. Gentamicin (Gm) was used at 1.25 μg/ml and 10 μg/ml and kanamycin was used at 5 μg/ml and 10 μg/ml for *R. capsulatus* SB1003 and *E. coli* strains, respectively. All enzymes used for DNA manipulation were purchased from New England Biolabs (Ipswich, MA).

Analytical methods. (i) Ferrozine assay. A sterile syringe was used to withdraw and transfer ~200 μl of sample from anaerobic cultures into the wells of a 96-well plate (Becton Dickinson, Franklin Lakes, NJ). Ten microliters of this aliquot was immediately transferred, in triplicate, into wells containing 90 μl of 1 N HCl. One hundred microliters of 0.1% ferrozine in 50% ammonium acetate was added, mixed, and allowed to incubate at room temperature for 10 min. The absorbance at 570 nm was measured. A standard curve for Fe(II), prepared over the range of 0.5 to 4 mM, was used to calculate the Fe(II) sample concentration.

(ii) Cell suspension assay. All cell suspension assays were prepared and conducted at room temperature in an anaerobic chamber containing an atmosphere of 5% H_2:80% N_2:15% CO_2 and incubated in the presence or absence of light as indicated. Cells were pregrown in FEM plus H_2 until mid-exponential phase (optical density at 600 nm of ~0.3), 8 ml of culture was harvested and washed in an equal volume of assay buffer (50 mM HEPES [*N*-2-hydroxyethylpiperazine-*N*′-2-ethanesulfonic acid] and 20 mM NaCl at pH 7) and resuspended in assay buffer containing 0.4 to 0.6 mM $FeCl_2$ and 20 mM $NaHCO_3$, and 100-μl aliquots were dispensed in 96-well plates. The Fe(II) concentration was measured as a function of time by adding 100 μl of ferrozine reagent to the samples and measuring the absorbance at 570 nm.

(iii) Protein assay. A sterile syringe was used to withdraw 1 ml of sample from anaerobic cultures and transfer it to a 2-ml microcentrifuge tube containing 800 μl oxalate solution (28 g of ammonium oxalate and 15 g of oxalic acid per liter) and 100 μl of 100 mM ferrous ethylenediammonium sulfate. The contents were mixed by vortexing for 30 s and then incubated at 37°C for 30 min for mineral dissolution. Total protein was precipitated by the addition of 75 μl of 10 M trichloroacetic acid, vortexing, and incubating on ice for 30 min. Precipitated protein was collected by centrifugation (16,000 × *g* for 15 min) at 4°C. The pellet was resuspended in 500 μl of 0.1 N NaOH and boiled for 5 min. In triplicate, 160 μl of the cooled sample was mixed with 40 μl of Bradford reagent and the samples were processed as prescribed by the manufacturer (Bio-Rad, Hercules, CA).

(iv) High-pressure liquid chromatography (HPLC). A syringe was used to withdraw 0.5 ml of sample from anaerobic cultures and transfer it to a Spin-X 0.22-μm cellulose acetate filter (Costar; Corning, Inc., Corning NY), and the cells were removed by centrifugation at 16,000 × *g* for 10 min. Citrate, β-ketoglutarate, and acetoacetic acid were analyzed using an Aminex HPX-87H column (Bio-Rad, Hercules, CA) at 30°C. Phosphoric acid (30 mM, pH 1.2) was used as the mobile phase, and absorbance was monitored at 210 nm with a UV detector.

Molecular techniques. Cloning was carried out in *E. coli* UQ950 by standard methods (2), and constructs were mated into *R. capsulatus* SB1003 by using *E. coli* WM3064. Annotated sequences of the *R. capsulatus* SB1003 genome were obtained using Ergo Light from the *R. capsulatus* SB1003 genome available through Integrated Genomics.

(i) In-frame deletion of *hupS* and *hupL*. A knockout construct for the *R. capsulatus* SB1003 *hupS* and *hupL* genes was generated by using yeast gap repair cloning to insert ~1 kb of DNA flanking the 5′ and 3′ regions of *hupS* and *hupL* into pMQ30 using the primers listed in Table 1. The plasmid pMQ30 is a *sacB*-based allelic exchange vector for gram-negative bacteria that cannot support the ColE1 origin of replication and contains *CEN6/ARSH4* DNA sequences to support replication in yeast (*Saccharomyces cerevisiae*) and a *URA3* yeast selectable marker (35). Primers pnc001 and pnc002 were used to amplify the 5′-flanking DNA, and primers pnc003 and pnc004 were used to amplify the 3′-flanking DNA. The 5′ and 3′ flanking fragments were cloned in vivo into pMQ30 using the *S. cerevisiae* uracil auxotrophic strain InvSc1 (Invitrogen, Carlsbad, CA) as previously described (7, 15), resulting in pNC001. Transformants that had undergone gap repair cloning and inserted the DNA fragments into pMQ30 by homologous recombination were selected on medium lacking uracil, and plasmids were isolated and transformed into *E.* coli UQ950 as previously described (7, 23).

The native *sacB* promoter found on pMQ30 did not express in *R. capsulatus* SB1003; therefore, primers pnc017 and pnc018 were used to amplify the knockout fragment of *hupS* and *hupL* from pNC001 and the amplified fragment was digested using engineered restriction sites (SacI and XbaI) and ligated into pZJD29a (J. Jiang and C. E. Bauer, unpublished plasmid construction) and digested with SacI and XbaI, resulting in pNC005. We electroporated the plasmid into *E. coli* WM3064 and mated it into *R. capsulatus* SB1003, selecting for Gm resistance. Resolution of the integrated plasmid was performed by selection on 5% sucrose, followed by PCR-based screening for loss of the wild-type gene.

(ii) Construction of a yeast-based allelic exchange vector for phototrophic bacteria. Plasmid pNC006 is a *sacB*-based allelic exchange vector for gram-negative bacteria that cannot support the ColE1 origin of replication but can be maintained in *S. cerevisiae* and *E. coli*. Plasmid pNC006 was built by cloning a copy of the *sacB* gene under the control of a native *R. capsulatus* promoter into pMQ87 using yeast gap repair cloning as described above. Plasmid pMQ87 is a suicide vector for gram-negative bacteria and contains the *CEN6/ARSH4* DNA sequences for replication in yeast and a *URA3* yeast selectable marker (35). It was linearized with the restriction enzyme XhoI. Primers pnc021 and pnc022 were designed to amplify a 2-kb fragment from pZJD29a containing the *sacB* gene under control of the *R. capsulatus pucAB* promoter. The digested plasmid (pMQ87) and the PCR fragment were cotransformed into *S. cerevisiae* InvSc1 (Invitrogen) as described above. Yeast transformants that had inserted the PCR fragment into pMQ87 by gap repair homologous recombination, resulting in pNC006, were selected as described above.

(iii) In-frame deletion of RRC00247 and RRC00248. Plasmid pNC007 was constructed using yeast gap repair cloning as described above. Briefly, primers pnc023 and pnc027 were used to amplify the 5′-flanking DNA fragment, and primers pnc026 and pnc028 were used to amplify the 3′-flanking DNA fragment. The 5′ and 3′ flanking DNA fragments and pNC006 linearized with BamHI were cotransformed into *Saccharomyces cerevisiae*, and homologous recombination events leading to the formation of pNC007 were selected for as described above. The plasmids were mated into *R. capsulatus* SB1003 and the resulting integrants, and resolved mutants were determined as described above.

(iv) Construction of RRC00247 and RRC00248 complementation plasmid. Primers pnc033 and pnc034 were designed ~500 bp upstream and downstream of the RRC00247 and RRC00248 operon. The primers were engineered to create a PCR fragment that could be digested with SacI and XbaI and ligated into pMQ131 digested with those same enzymes. Plasmid pMQ131 is a broad host range plasmid designed for cloning using the yeast gap repair system (R. M. Q. Shanks and G. A. O'Toole, unpublished data; www.dartmouth.edu/~gotoole/vectors.html). This construct presumably carries the native RRC00247 and RRC00248 promoter.

RESULTS

Anoxygenic phototrophic Fe(II) oxidation by *R. capsulatus* SB1003. Fig. 1A and a previous report from our lab (10) show that whole-cell suspensions of *R. capsulatus* SB1003 possess light-dependent Fe(II) oxidation activity. In this assay, cells from H_2-grown, exponential phase cultures are washed and resuspended in medium containing soluble Fe(II) and the ability of the cell suspension to oxidize Fe(II) is measured as a function of time using the ferrozine assay. Total iron [Fe(II) + Fe(III)] remains constant through these experiments (data not shown). The oxidation of Fe(II) is independent of cell growth due to the short time scale of this assay (less than 3 h) (Fig. 1A) and the large number of cells present in the suspension (see Materials and Methods). Thus, this assay measures only the ability of an organism to oxidize Fe(II) and is not a measure of

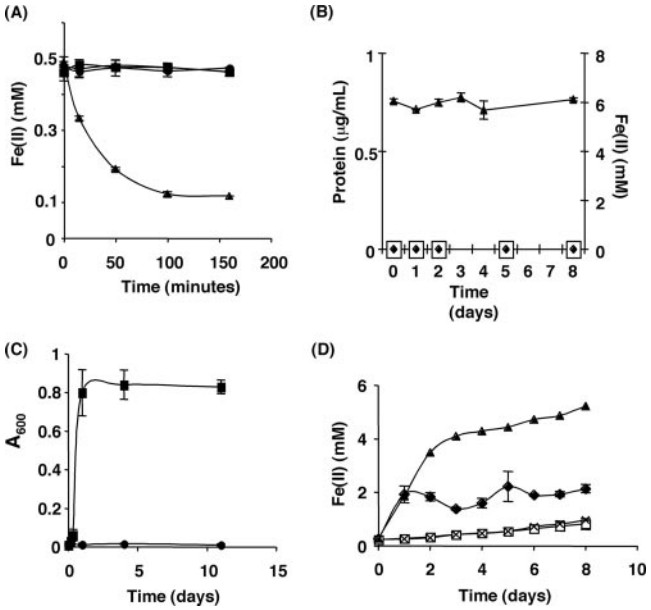

FIG. 1. Anoxygenic phototrophic Fe(II) oxidation and phototrophic growth on Fe(III)-citrate by *R. capsulatus* SB1003. (A) *R. capsulatus* SB1003 can perform phototrophic Fe(II) oxidation. A cell suspension assay was performed in medium containing 0.5 mM Fe(II). ▲, *R. capsulatus* SB1003 in the light; ●, *R. capsulatus* SB1003 in the dark; ■, uninoculated control in the light. (B) *R. capsulatus* SB1003 cannot grow by Fe(II) oxidation. Protein concentration and Fe(II) concentration were measured over time for cells incubated in the presence of 4 to 6 mM Fe(II). □, *R. capsulatus* SB1003 in the light; ◆, uninoculated control in the light; ▲, Fe(II) concentration of the *R. capsulatus* SB1003 cultures. (C) *R. capsulatus* SB1003 cannot use citrate as a phototrophic carbon source. Cells were incubated in medium containing 10 mM citrate (●) or 10 mM acetate (■) and assayed for growth. (D) Phototrophic growth of *R. capsulatus* SB1003 in the presence of Fe(II)-citrate. Cells were incubated in medium containing 5 mM Fe(III) and 10 mM citrate. Uninoculated controls were prepared and incubated similarly. Over time, aliquots were removed and Fe(II) concentrations were measured. End point protein concentrations were determined for inoculated samples. ◆, *R. capsulatus* SB1003 in the light (final protein concentration of ~139 μg/ml); ×, *R. capsulatus* SB1003 in the dark (final protein concentration was below detection); ▲, uninoculated control in the light; □, uninoculated control in the dark. Error bars in panels A, B, C, and D show the standard deviations of triplicate cultures.

an organism's ability to grow via anoxygenic phototrophic Fe(II) oxidation.

To test whether *R. capsulatus* SB1003 could grow via anoxygenic phototrophic Fe(II) oxidation, cells from H_2-grown cultures were diluted in medium containing ~6 mM Fe(II) as the sole electron source. Although *R. capsulatus* SB1003 possessed light-dependent Fe(II) oxidation activity (Fig. 1A), it did not exhibit photoautotrophic growth on Fe(II) (Fig. 1B). Over the course of 8 days, the protein concentration of the Fe(II) cultures inoculated with *R. capsulatus* SB1003 was identical to that of the uninoculated media controls and remained below the detection limit of the protein assay used (Fig. 1B). In addition, the Fe(II) concentration (Fig. 1B) remained ~6 mM throughout the time course of the experiment, indicating that appreciable Fe(II) oxidation did not occur in the presence of the small amount of cells that are incapable of growth on Fe(II).

Phototrophic growth of *R. capsulatus* SB1003 on Fe(III)-citrate. *R. capsulatus* SB1003 is able to oxidize iron (Fig. 1A) but cannot grow photoautotrophically when Fe(II) is provided as the sole electron source (Fig. 1B). This fact led us to speculate about alternative functions for Fe(II) oxidation in this organism. One explanation for the Fe(II) oxidation activity is that it provides a mechanism for organic carbon acquisition. In numerous environments, iron exists in chelated forms and many Fe(III)-chelates are subject to light-induced photoredox reactions that result in the reduction of Fe(III) and the degradation of the chelator (4, 5). We hypothesized that microbially catalyzed Fe(II) oxidation, coupled with ferrated-ligand photochemistry, could convert otherwise inaccesible pools of carbon into labile substrates capable of supporting microbial growth.

To test this hypothesis, citrate was chosen as a model carbon source because it has been reported to not be metabolized by *R. capsulatus* SB1003 under anoxygenic phototrophic conditions (41) and it is also subject to photochemistry in the presence of Fe(III) (1). Our hypothesis predicts that microbially catalyzed Fe(II) oxidation in the presence of citrate will lead to the formation of Fe(III)-citrate, and that the latter will undergo photochemical degradation to produce a carbon source(s) that can sustain growth. We confirmed that *R. capsulatus* SB1003 cannot use citrate as a carbon source for photoheterotrophic growth under the culture conditions used in this study, whereas it can use acetate as a carbon source for photoheterotrophic growth (Fig. 1C). The above hypothesis also requires Fe(III)-citrate photochemistry to occur under our culture conditions. To test whether this requirement was met, we incubated uninoculated medium containing Fe(III)-citrate in the presence or absence of light and measured the reduction of Fe(III) using the ferrozine assay (Fig. 1D). The concentration of Fe(II) rapidly increased [indicating a reduction in Fe(III)] to ~4 mM during the first 2 days of incubation for uninoculated medium exposed to light, and over the next 6 days, the concentration slowly approached ~6 mM. In contrast, the Fe(II) levels in the nonilluminated uninoculated medium remained below 1 mM for the duration of the experiment. These data indicated that Fe(III)-citrate photochemistry that results in the production of Fe(II) can occur in our experimental system.

The next prediction of our hypothesis is that *R. capsulatus* SB1003 should be able to use Fe(III)-citrate as a carbon source in a light-dependent manner. To test this prediction, cells from H_2-grown cultures were diluted in medium containing Fe(III)-citrate and incubated in the presence or absence of light. Over the course of the experiment, the protein concentration of the cultures exposed to light increased from levels that were undetectable at day 0 to levels of ~139 μg/ml by day 8. Protein concentration remained undetectable in cultures incubated in the dark. This result indicated that *R. capsulatus* SB1003 can grow on Fe(III)-citrate in a light-dependent manner.

In addition to protein level, the Fe(II) concentrations of the illuminated and nonilluminated SB1003 cultures supplemented with Fe(III)-citrate were monitored as a function of time (Fig. 1D). The concentration of Fe(II) increased slightly in nonilluminated cultures but was not significantly different from the nonilluminated uninoculated medium, indicating a low level of Fe reduction in the system that is independent of

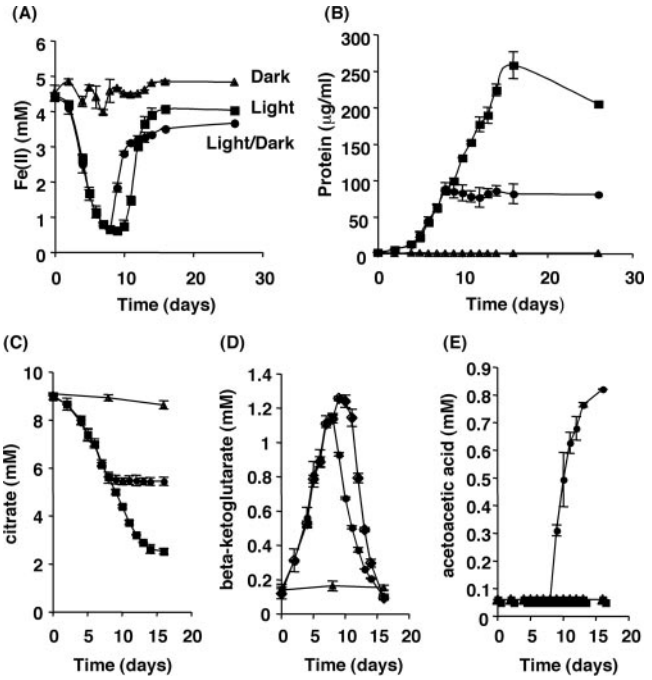

FIG. 2. Phototrophic growth of *R. capsulatus* SB1003 on Fe(II)-citrate. Cells were incubated in medium containing 4 to 6 mM Fe(II) and 10 mM citrate in the light (■), dark (▲), or in the light and shifted to the dark on day 7 (●). Over time, aliquots were removed and Fe(II) (A), protein (B), citrate (C), β-ketoglutarate (D), and acetoacetic acid (E) concentrations were measured. Error bars show the standard deviations of triplicate cultures.

the bacteria present. When Fe(III)-citrate-containing cultures were incubated in the light, a rapid increase in the Fe(II) concentration was observed within the first 24 h, after which the concentration of Fe(II) stabilized. Our assay conditions take into account intracellular Fe(II) as well as cell-associated Fe(II). Therefore, the different levels of Fe(II) achieved between illuminated SB1003 cultures and uninoculated media incubated in the light are not a result of cellular Fe(II) consumption. This result suggests that the concentration of Fe(II) in the illuminated cultures is dependent mainly on a combination of the rate of abiotic, light-dependent Fe(III) reduction and the rate of bacterial Fe(II) oxidation.

Phototrophic growth of *R. capsulatus* SB1003 on Fe(II)-citrate. After showing that *R. capsulatus* SB1003 can grow phototrophically on Fe(III)-citrate, our next objective was to determine whether the light-dependent Fe(II) oxidation activity of this organism, depicted in Fig. 1A, could support growth through the generation of Fe(III)-citrate from Fe(II)-citrate. Cells from H_2-grown cultures were diluted in medium containing ~4 to 5 mM Fe(II) and 10 mM citrate and incubated under light regimens consisting of constant illumination, constant darkness, or constant illumination initially for 7 days, followed by constant darkness for the duration of the experiment (Fig. 2). Aliquots were removed from the cultures at various time points, and the Fe(II) concentration (Fig. 2A) and the protein concentration (Fig. 2B) were measured.

In the absence of light, Fe(II) concentrations remained ~4.5 mM for the duration of the experiment, indicating that little or no Fe(II) oxidation occurred in the dark. In the presence of light, the initial rate of Fe oxidation that occurred over the first 2 days was low and was followed by an increased rate of Fe oxidation that lasted through day 8. During this time period, the Fe(II) concentration in the cultures decreased from ~4.4 mM to ~0.6 mM, demonstrating that Fe(II) oxidation in the presence of citrate is light dependent and consistent with the findings seen in the cell suspension assay (Fig. 1A). For cultures kept in constant light, the Fe(II) concentration remained ~0.6 mM from day 8 to day 10. At this point, the Fe(II) concentration began to increase and eventually leveled at ~4.0 mM by day 14.

To test whether the Fe(III) reduction that occurred from day 10 to day 14 was light dependent, we transferred phototrophically grown cultures to dark conditions after the Fe(II) oxidation phase (day 7) and the concentration of Fe(II) was measured as a function of time. While cultures left continuously in the light maintained Fe(II) concentrations at ~0.6 mM through day 10, the cultures that were moved to the dark showed an immediate Fe(III) reduction and the Fe(II) concentration increased to ~2.8 mM by day 10 and continued to increase until eventually leveling off at ~3.5 mM. Thus, the Fe(III) reduction observed in continuously illuminated cultures beyond day 7 cannot be solely accounted for by photochemical reactions and could be catalyzed by a light-independent bacterial process. In fact, strains of *R. capsulatus* have been shown to exhibit Fe(III) reduction that is not coupled to growth, although the mechanism is unknown (12).

Bacterial growth on Fe(II)-citrate was measured in terms of protein concentration (μg/ml) and is depicted in Fig. 2B. No increase in biomass was observed in cultures incubated in constant darkness. For phototrophic cultures, slow growth was observed for the first 4 days before an increase in biomass occurred. In cultures incubated under constant light, growth occurred during both the Fe(II) oxidation phase (day 0 to day 9) as protein levels reached ~100 μg/ml and during the Fe(III) reduction phase (day 10 to day 14) as protein levels continued to increase and reached ~250 μg/ml. This result indicated that anaerobic growth on Fe(II)-citrate is a phototrophic process during the Fe(II) oxidation phase.

The protein concentration of cultures incubated in the light during the Fe(II) oxidation phase (day 0 to day 7) and then transferred to the dark during the Fe reduction phase (day 8 to day 16) revealed that biomass increased (to ~100 μg/ml) only in the presence of light (day 0 to day 7) and growth ceased upon transfer to the dark (day 8 to day 16). This result indicated that the growth seen during the Fe(III) reduction phase (day 8 to day 14) is light dependent and that the Fe(III) reduction observed during the dark incubation cannot support anaerobic growth of *R. capsulatus* SB1003 under these conditions.

Fe-citrate photochemistry and the formation of potential carbon sources for photoheterotrophic growth. It is well documented that the initial photochemistry occurring between Fe(III) and citrate leads to the reduction of Fe(III) and the oxidation of citrate yielding Fe(II) and β-ketoglutarate (1, 16) according to the following reaction: citrate + $2Fe^{3+}$ + hν → β-ketoglutarate + CO_2 + $2Fe^{2+}$ + $2H^+$. In an aqueous environment, β-ketoglutarate spontaneously undergoes light-independent decarboxylation, producing acetoacetic acid (i.e.,

β-ketoglutarate → acetoacetate + CO_2) (1, 16). Our hypothesis predicts that β-ketoglutarate and/or acetoacetic acid should be present in the supernatant of *R. capsulatus* SB1003 cultures growing on Fe(II)-citrate and that one or both of these compounds can support the growth of this organism under phototrophic conditions.

To test this prediction, in addition to measuring the Fe(II) and protein concentrations of Fe(II)-citrate cultures grown under various light regimens (Fig. 2A and B), we also measured the concentrations of the suspected carbon intermediates using HPLC (citrate [Fig. 2C], β-ketoglutarate [Fig. 2D], acetoacetic acid [Fig. 2E]). In cultures maintained in constant darkness, the citrate concentration remained constant (~9 mM) for the duration of the experiment, while β-ketoglutarate and acetoacetic acid were not detected. In contrast, the citrate concentration steadily decreased from ~9 mM to ~2.5 mM in cultures subjected to light. In these cultures, the β-ketoglutarate concentration steadily increased to ~1.25 mM by day 9 and then steadily decreased to below detection by day 16. Acetoacetic acid was not detected in the illuminated cultures.

In cultures initially subjected to constant light, the citrate concentration decreased from ~9 mM to ~5.5 mM during the light phase (day 0 to day 7) and leveled off upon transfer to the dark phase (day 8 to day 16). The β-ketoglutarate concentration of these cultures steadily increased to ~1.15 mM during exposure to the light and then steadily decreased to below the limit of detection upon transfer to constant darkness. Acetoacetic acid was not detected in these cultures during exposure to light and accumulated only when cultures were transferred to constant darkness, steadily increasing to ~0.8 mM by the end of the experiment.

The genes RRC00247 and RRC00248 are required for optimal growth on Fe(III)-citrate. Bacterial growth on Fe(II)-citrate occurs only in the presence of light (Fig. 2B). During this time period, β-ketoglutarate accumulated (Fig. 2D), while acetoacetic acid could not be detected (Fig. 2E). Acetoacetic acid concentrations build to detectable levels only when cultures are shifted from light to dark, which is a condition that leads to growth cessation (Fig. 2B and E). The fact that acetoacetic acid accumulated only after growth ceased suggested that this intermediate, and not β-ketoglutarate, was the labile carbon source capable of supporting phototrophic growth of *R. capsulatus* SB1003 when grown on Fe(II)-citrate or Fe(III)-citrate.

A genetic approach was taken to test whether acetoacetic acid was indeed the carbon source used by *R. capsulatus* SB1003 under these conditions. An in-frame deletion of the genes RRC00247 and RRC00248 was constructed on the chromosome of *R. capsulatus* SB1003. The genes RRC00247 and RRC00248 encode proteins that are homologous to the *E. coli* proteins AtoD and AtoA, respectively. At the amino acid level, AtoD and RRC00247 are 42.3% identical and AtoA and RRC00248 are 49.8% identical. In *E. coli*, these proteins are involved in the utilization of acetoacetic acid. The proteins AtoA and AtoD form the acetyl-CoA–acetoacetyl-CoA transferase, which catalyzes the conversion of acetoacetic acid into acetoacetyl-CoA (36). The latter is converted to acetyl-CoA by the acetyl-CoA acetyltransferase encoded in *E. coli* by the *atoB* gene (13). In comparison to the wild-type strain, no growth defect was observed when the *R. capsulatus* SB1003 ΔRRC00247-RRC00248 (encoding homologs of AtoA and AtoD) mutant was grown under photoheterotrophic conditions on acetate or under photoautotrophic conditions on H_2 (data not shown). However, when the *R. capsulatus* SB1003 ΔRRC00247-RRC00248 mutant was grown phototrophically on Fe(III)-citrate and carried pMQ131 (empty vector control), a growth defect was observed relative to the wild-type carrying pMQ131 (Fig. 3). The growth defect could be complemented through the introduction of a plasmid containing RRC00247 and RRC00248 (pNC008) into the *R. capsulatus* SB1003 ΔRRC00247-RRC00248 mutant (Fig. 3). This plasmid (pNC008) did not significantly alter the ability of the wild-type strain to grow on Fe(III)-citrate (Fig. 3). These data indicate that acetoacetic acid is the primary growth substrate for *R. capsulatus* SB1003 when grown on Fe(III)-citrate or Fe(II)-citrate under phototrophic conditions.

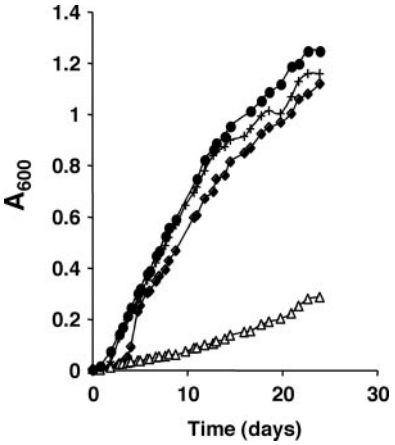

FIG. 3. Acetoacetic acid utilization is required for optimal growth of *R. capsulatus* SB1003 on Fe(III)-citrate. Wild-type *R. capsulatus* SB1003 and a mutant with a deletion of two genes (RRC00247 and RRC00248) involved in utilization of acetoacetic acid were tested for photoheterotrophic growth in the presence of Fe(III)-citrate. Cultures were incubated in medium containing 5 mM Fe(III) and 10 mM citrate in the light, and the absorbance at 600 nm was measured over time. ◆, wild-type/pMQ131 (vector control); +, wild-type/pNC008 (with RRC00247 to RRC00248); △, ΔRRC00247-RRC00248/pMQ131 (vector control); ●, ΔRRC00247-RRC00248/pNC008 (with RRC00247 to RRC00248). Data are representative of triplicate cultures.

Other Fe(II) complexes tested for phototrophic growth of *R. capsulatus* SB1003. To explore whether there were other examples of Fe(II) oxidation serving as a mechanism for carbon acquisition, we tested other Fe chelators at concentrations of 10 to 20 mM. The addition of EDTA to the Fe(II) medium did not lead to cell growth but led to technical difficulties with Fe(II) detection because it functioned as a better Fe(II) chelator than the ferrozine reagent did. The addition of oxalate to the Fe(II) medium caused the precipitation of medium components, making its effects on Fe(II) oxidation and growth difficult to interpret. In the absence of Fe(II), *R. capsulatus* SB1003 was able to grow photoheterotrophically on glutamate; thus, this chelator could not be used to test our hypothesis. However, similarly to the case with Fe(II)-citrate, light-dependent growth and light-dependent Fe(II) oxidation were observed in the presence of Fe(II)-NTA.

The uptake hydrogenase does not function as the Fe(II) oxidoreductase. Photoautotrophic growth on H_2 requires an uptake hydrogenase. It has been postulated that this enzyme could oxidize Fe(II) under more reducing conditions, such as in the presence of a chelator (45). Therefore, we constructed an in-frame deletion of the genes (*hupS* and *hupL*) that encode the subunits of the uptake hydrogenase in *R. capsulatus* SB1003 (9, 29). As expected, the mutant lacking *hupS* and *hupL* was unable to grow photoautotrophically on H_2 (data not shown), but in the presence of NTA, this mutant was able to oxidize Fe(II) and produce levels of biomass indistinguishable from those of the wild-type strain (data not shown), indicating that the uptake hydrogenase of *R. capsulatus* SB1003 does not function as the Fe(II) oxidoreductase.

DISCUSSION

Microbially catalyzed Fe(II) oxidation, whether occurring in oxic or anoxic environments, at a neutral or acidic pH, or in the presence or absence of light, is generally accepted as a lithoautotrophic mode of growth (for a recent review, see the work of Weber et al. at reference 42). In this report, we have taken the initial steps in characterizing a new role for microbially catalyzed Fe(II) oxidation: one that supports organic carbon acquisition.

Using *R. capsulatus* SB1003 as an example of what we suspect may be true for many other Fe(II)-oxidizing bacteria, we have shown that it can oxidize soluble Fe(II) but cannot use soluble Fe(II) to support a lithotrophic metabolism based on photoautotrophic Fe(II) oxidation (Fig. 1A and B). Instead, *R. capsulatus* SB1003 exploits Fe(II) oxidation to access organic carbon sources (e.g., citrate and NTA) that it could not use otherwise. A model of this exploitation is shown in Fig. 4. *R. capsulatus* SB1003 cannot grow on either soluble Fe(II) (Fig. 1B) or citrate (Fig. 1C) alone. However, it can grow phototrophically if both Fe(II) and citrate are provided in the medium (Fig. 2B). Growth is dependent upon microbially catalyzed Fe(II) oxidation (Fig. 2A) leading to the formation of Fe(III)-citrate, which, through consecutive photochemical and spontaneous decarboxylation reactions, is converted into acetoacetic acid (Fig. 2C to E). A mutant with a chromosomal deletion of genes essential for acetoacetic acid utilization (ΔRRC00247-RRC00248) has a severe growth defect on Fe(III)-citrate, indicating that during the breakdown of Fe(III)-citrate, carbon is primarily assimilated through the incorporation of acetoacetic acid (Fig. 3). In this fashion, *R. capsulatus* SB1003 is able to support photoheterotrophic growth on an otherwise nonutilizable carbon source as a result of Fe(II) oxidation. To our knowledge, this is the first example of an organism benefiting from Fe(II) oxidation in this fashion.

Although it is possible that citrate may facilitate photoautotrophic growth by altering the redox potential or by preventing cell encrustation, our data indicate that Fe(II) oxidation is coupled to photoheterotrophic growth. This indication is supported by the following logic. For a metabolism based on photoautotrophic Fe(II) oxidation, the maximum theoretical yield of protein produced per mole of soluble Fe(II) oxidized based on the stoichiometry of CO_2 reduction coupled to Fe(II) oxidation is ~3.5 g/mol (25) according to the following equation: $4\ Fe^{2+} + HCO_3^- + 10\ H_2O = <CH_2O> + 7\ H^+ + 4$

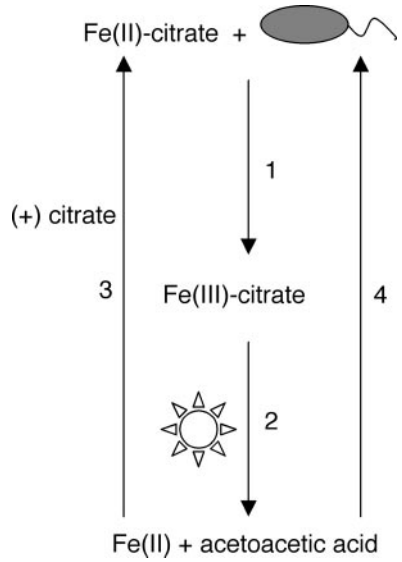

FIG. 4. Model for Fe(II) oxidation leading to carbon acquisition. In the presence of Fe(II)-citrate, *R. capsulatus* SB1003 is able to oxidize Fe(II) leading to the formation of Fe(III)-citrate (arrow 1). In the presence of light, Fe(III)-citrate undergoes a photochemical reaction yielding Fe(II) and β-ketoglutarate and the latter spontaneously decarboxylates into acetoacetic acid (arrow 2). As a result of the photochemical reaction, the resulting Fe(II) can become bound by citrate (arrow 3) and microbially reoxidized. The acetoacetic acid that results from these reactions can be used as a carbon source for growth (arrow 4).

$Fe(OH)_3$. When *R. capsulatus* SB1003 was grown on Fe(II)-citrate, more than 200 μg/ml of protein was produced at the expense of ~5 mM of Fe(II), corresponding to a molar growth yield (~20 g/mol) that is five times greater than the theoretical maximum for anoxygenic photoautotrophic Fe(II) oxidation. Thus, the growth achieved under these conditions cannot be a result of chelator-facilitated photoautotrophic Fe(II) oxidation and is best explained by Fe(II) oxidation leading to citrate breakdown and eventual photoheterotrophic growth on acetoacetic acid. In agreement with this explanation, the *R. capsulatus* SB1003 ΔRRC00247-RRC00248 mutant, which lacks homologs of genes involved in acetoacetic acid utilization (*atoAD*), was severely defective for growth on Fe(III)-citrate (Fig. 3).

We are further investigating additional organic ligands to determine whether they have the same effect as citrate. Of particular interest is the fact that *R. capsulatus* SB1003 can also grow on Fe(II)-NTA. We propose that coupling the Fe(II) oxidation activity of *R. capsulatus* SB1003 with Fe(III)-NTA photochemistry degrades recalcitrant NTA into a labile carbon source, analogous to what occurs for Fe(III)-citrate. Fe(III)-NTA photochemistry is well documented in the literature, and the expected products are Fe(II), iminodiacetate, formaldehyde, and CO_2 (37, 40). Based on the presence of a gene annotated as a glutathione-dependent formaldehyde dehydrogenase (RRC01948) in the sequenced genome of *R. capsulatus* SB1003, we predict that the growth on Fe(II)-NTA occurs as a result of Fe(II) oxidation and Fe(III)-NTA photochemistry leading to the production of formaldehyde. Glutathione-dependent formaldehyde dehydrogenases, such as FrmA in *E.*

coli, generate NAD(P)H through the oxidation of a substrate (*S*-hydroxymethylglutathione) produced by the spontaneous reaction of formaldehyde and glutathione (19). Whether this is also the case for *R. capsulatus* SB1003 remains to be shown.

Our data demonstrating that microbial Fe(II) oxidation can lead to carbon acquisition supports the previous notion that microbial metal oxidation can be used to break down pools of recalcitrant carbon. Sunda and Kieber showed that Mn(IV) oxides degrade humic and fulvic substances into low-molecular-weight organic compounds (pyruvate, acetone, acetaldehyde, and formaldehyde) (38), and it has been suggested that Mn(IV) oxides are deposited on the bacterial cell surface to lyse inaccessible organic material into potential growth substrates (39). As observed with Mn(IV) oxides, it has been shown that biologically catalyzed Fe(III) oxides also localize to the cell surface (22, 25) and, based on our findings, such localization could aid in the ability of cells to access extracellular pools of organic carbon. Determining whether Fe(II) oxidation can facilitate the utilization of humic and fulvic substances as carbon sources is a priority for future research.

In addition to the Fe(II)-oxidizing phototrophs, it will be interesting to examine other Fe(II)-oxidizing bacteria (e.g., aerobic/anaerobic, neutrophilic, and acidophilic) to determine whether Fe(II) oxidation is a widespread mechanism for organic carbon acquisition in the photic zone. We are encouraged by reports in the literature that other phototrophs may exhibit this behavior. For instance, *R. vannielii* is another example of an organism that cannot grow photoautotrophically on soluble Fe(II) but is able to simultaneously oxidize Fe(II) and grow in the presence of organic acids and chelators such as NTA (22). It is also noteworthy that the *R. vannielii* strain isolated in this study came from Fe(II) enrichment cultures that also contained trace amounts of organic material present in the inoculum. The authors concluded that although *R. vannielii* cannot grow photoautotrophically on Fe(II) alone, the ability of this organism to oxidize Fe(II) may be a selective advantage in nature as long as organic material is present (22). Based on our data, we speculate that Fe(II) oxidation in the presence of organic material can be a selective advantage leading to the photochemical breakdown of otherwise inaccessible organic compounds into suitable growth substrates. Of course, strict chemolithoautotrophs [such as certain aerobic acidophilic Fe(II) oxidizers] would not be expected to benefit from this process.

Our findings, in conjunction with those regarding Fe(III) ligand photochemistry in the open ocean (reviewed by Barbeau in reference 3), have implications for our understanding of the iron and carbon cycles and the effect that these cycles may have on one another in both past and present environments. Ancient Fe-based ecosystems rely on Fe(II)-oxidizing phototrophs as the primary producers and essential catalysts of Fe(II) oxidation. As discussed by Canfield et al., it is believed that a significant fraction of Fe(II) may have entered such systems though weathering and re-reduction of iron oxides resulting from phototrophic Fe(II) oxidation by Fe(III) reducing bacteria (8). Another layer that can be added to this model with respect to the re-reduction of Fe(III) is the photochemistry that can occur between Fe(III) and organic ligands. This alternative mechanism could promote iron cycling in the photic zone, the niche of Fe(II)-oxidizing phototrophs. Future work in both freshwater and marine environments will be necessary to test these predictions.

ACKNOWLEDGMENTS

We thank Yun Wang for expertise and technical assistance with HPLC. We also thank Yongqin Jiao and anonymous reviewers for their constructive comments on the manuscript.

This work was supported by grants from the Howard Hughes Medical Institute and Packard Foundation to D.K.N.

REFERENCES

1. **Abrahamson, H. B., A. B. Rezvani, and J. G. Brushmiller.** 1994. Photochemical and spectroscopic studies of complexes of iron(III) with citric-acid and other carboxylic-acid. Inorg. Chim. Acta **226:**117–127.
2. **Ausubel, F. M., R. Brent, R. E. Kingston, D. D. Moore, J. G. Seidman, J. A. Smith, and K. Struhl.** 1992. Current protocols in molecular biology. Wiley Interscience, New York, NY.
3. **Barbeau, K.** 2006. Photochemistry of organic iron(III) complexing ligands in oceanic systems. Photochem. Photobiol. **82:**1505–1516.
4. **Barbeau, K., E. L. Rue, K. W. Bruland, and A. Butler.** 2001. Photochemical cycling of iron in the surface ocean mediated by microbial iron(III)-binding ligands. Nature **413:**409–413.
5. **Barbeau, K., G. Zhang, D. H. Live, and A. Butler.** 2002. Petrobactin, a photoreactive siderophore produced by the oil-degrading marine bacterium *Marinobacter hydrocarbonoclasticus*. J. Am. Chem. Soc. **124:**378–379.
6. **Bertani, G.** 2004. Lysogeny at mid-twentieth century: P1, P2, and other experimental systems. J. Bacteriol. **186:**595–600.
7. **Burke, D., Dawson, D., and Stearns, T.** 2000. Methods in yeast genetics: a Cold Spring Harbor Laboratory course manual. Cold Spring Harbor Laboratory Press, Plainview, NY.
8. **Canfield, D. E., M. T. Rosing, and C. Bjerrum.** 2006. Early anaerobic metabolisms. Philos. Trans. R. Soc. Lond. B **361:**1819–1834.
9. **Cauvin, B., A. Colbeau, and P. M. Vignais.** 1991. The hydrogenase structural operon in *Rhodobacter capsulatus* contains a third gene, *hupM*, necessary for the formation of a physiologically competent hydrogenase. Mol. Microbiol. **5:**2519–2527.
10. **Croal, L. R., Y. Q. Jiao, and D. K. Newman.** 2007. The *fox* operon from *Rhodobacter* strain SW2 promotes phototrophic Fe(II) oxidation in *Rhodobacter capsulatus* SB1003. J. Bacteriol. **189:**1774–1782.
11. **Croal, L. R., C. M. Johnson, B. L. Beard, and D. K. Newman.** 2004. Iron isotope fractionation by Fe(II)-oxidizing photoautotrophic bacteria. Geochim. Cosmochim. Acta **68:**1227–1242.
12. **Dobbin, P. S., L. H. Warren, N. J. Cook, A. G. McEwan, A. K. Powell, and D. J. Richardson.** 1996. Dissimilatory iron(III) reduction by *Rhodobacter capsulatus*. Microbiology **142:**765–774.
13. **Duncombe, G. R., and F. E. Frerman.** 1976. Molecular and catalytic properties of the acetoacetyl-coenzyme A thiolase of *Escherichia coli*. Arch. Biochem. Biophys. **176:**159–170.
14. **Ehrenreich, A., and F. Widdel.** 1994. Anaerobic oxidation of ferrous iron by purple bacteria, a new type of phototrophic metabolism. Appl. Environ. Microbiol. **60:**4517–4526.
15. **Elble, R.** 1992. A simple and efficient procedure for transformation of yeasts. BioTechniques **13:**18–20.
16. **Frahn, J. L.** 1958. The photochemical decomposition of the citrate-ferric iron complex—a study of the reaction products by paper ionophoresis. Aust. J. Chem. **11:**399–405.
17. **Garrels, R. M., and E. A. Perry, Jr.** 1974. Cycling of carbon, sulfur, and oxygen through geologic time, p. 303–336. *In* E. D. Goldberg (ed.), The sea, vol. 5. Wiley, New York, NY.
18. **Gledhill, M., and C. M. G. Vandenberg.** 1994. Determination of complexation of iron(III) with natural organic complexing ligands in seawater using cathodic stripping voltammetry. Mar. Chem. **47:**41–54.
19. **Gutheil, W. G., E. Kasimoglu, and P. C. Nicholson.** 1997. Induction of glutathione-dependent formaldehyde dehydrogenase activity in *Escherichia coli* and *Hemophilus influenza*. Biochem. Biophys. Res. Commun. **238:**693–696.
20. **Hartman, H.** 1984. The evolution pf photosynthesis and microbial mats: a speculation on the banded iron formations, p. 449–453. *In* Y. Cohen, R. W. Castenholz, and H. O. Halvorson (ed.), Microbial mats: stromatolites. Alan R. Liss, Inc., New York, NY.
21. **Heising, S., L. Richter, W. Ludwig, and B. Schink.** 1999. *Chlorobium ferrooxidans* sp. nov., a phototrophic green sulfur bacterium that oxidizes ferrous iron in coculture with a "*Geospirillum*" sp. strain. Arch. Microbiol. **172:**116–124.
22. **Heising, S., and B. Schink.** 1998. Phototrophic oxidation of ferrous iron by a *Rhodomicrobium vannielii* strain. Microbiology **144:**2263–2269.
23. **Hoffman, C. S., and F. Winston.** 1987. A ten-minute DNA preparation from yeast efficiently releases autonomous plasmids for transformation of *Escherichia coli*. Gene **57:**267–272.

24. **Ito, Y., and A. Butler.** 2005. Structure of synechobactins, new siderophores of the marine cyanobacterium *Synechococcus* sp. PCC 7002. Limnol. Oceanogr. **50:**1918–1923.
25. **Jiao, Y. Y. Q., A. Kappler, L. R. Croal, and D. K. Newman.** 2005. Isolation and characterization of a genetically tractable photoautotrophic Fe(II)-oxidizing bacterium, *Rhodopseudomonas palustris* strain TIE-1. Appl. Environ. Microbiol. **71:**4487–4496.
26. **Kappler, A., C. Pasquero, K. Konhauser, and D. K. Newman.** 2005. Deposition of banded iron formations by phototrophic Fe(II)-oxidizing bacteria. Geology **33:**865–868.
27. **Kuma, K., J. Nishioka, and K. Matsunaga.** 1996. Controls on iron(III) hydroxide solubility in seawater: the influence of pH and natural organic chelators. Limnol. Oceanogr. **41:**396–407.
28. **Küpper, F. C., C. J. Carrano, J. U. Kuhn, and A. Butler.** 2006. Photoreactivity of iron(III)-aerobactin: photoproduct structure and iron(III) coordination. Inorg. Chem. **45:**6028–6033.
29. **Leclerc, M., A. Colbeau, B. Cauvin, and P. M. Vignais.** 1988. Cloning and sequencing of the genes encoding the large and the small subunits of the H_2 uptake hydrogenase (hup) of *Rhodobacter capsulatus*. Mol. Gen. Genet. **214:**97–107.
30. **Martin, J. D., Y. Ito, V. V. Homann, M. G. Haygood, and A. Butler.** 2006. Structure and membrane affinity of new amphiphilic siderophores produced by *Ochrobactrum* sp. SP18. J. Biol. Inorg. Chem. **11:**633–641.
31. **Olson, J. M.** 2001. "Evolution of photosynthesis" (1970), re-examined thirty years later. Photosynth. Res. **68:**95–112.
32. **Olson, J. M.** 1970. The evolution of photosynthesis. Science **168:**438–446.
33. **Olson, J. M., and R. E. Blankenship.** 2004. Thinking about the evolution of photosynthesis. Photosynth. Res. **80:**373–386.
34. **Rue, E. L., and K. W. Bruland.** 1995. Complexation of iron(III) by natural organic-ligands in the central North Pacific as determined by a new competitive ligand equilibration adsorptive cathodic stripping voltammetric method. Mar. Chem. **50:**117–138.
35. **Shanks, R. M., N. C. Caiazza, S. M. Hinsa, C. M. Toutain, and G. A. O'Toole.** 2006. *Saccharomyces cerevisiae*-based molecular tool kit for manipulation of genes from gram-negative bacteria. Appl. Environ. Microbiol. **72:**5027–5036.
36. **Sramek, S. J., and F. E. Frerman.** 1975. Purification and properties of *Escherichia coli* coenzyme A-transferase. Arch. Biochem. Biophys. **171:** 14–26.
37. **Stolzberg, R. J., and D. N. Hume.** 1975. Rapid formation of iminodiacetate from photochemical degradation of iron(III) nitrilotriacetate solutions. Environ. Sci. Technol. **9:**654–656.
38. **Sunda, W. G., and D. J. Kieber.** 1994. Oxidation of humic substances by manganese oxides yields low-molecular-weight organic substrates. Nature **367:**62–64.
39. **Tebo, B. M., D. B. Edwards, W. G. Sunda, and D. J. Kieber.** 1995. Bacterial manganese oxidation leads to the degradation and utilization of natural organic-matter. Abstr. Pap. Am. Chem. Soc. **209:**77.
40. **Trott, T., R. W. Henwood, and C. H. Langford.** 1972. Sunlight photochemistry of ferric nitrilotriacetate complexes. Environ. Sci. Technol. **6:**367–368.
41. **Trueper, H. G., and N. Pfennig.** 1978. Taxonomy of the *Rhodospirillales*, p. 19–27. *In* R. K. Clayton and W. R. Sistrom (ed.), The photosynthetic bacteria. Plenum Press, New York, NY.
42. **Weber, K. A., L. A. Achenbach, and J. D. Coates.** 2006. Microorganisms pumping iron: anaerobic microbial iron oxidation and reduction. Nat. Rev. Microbiol. **4:**752–764.
43. **Widdel, F., S. Schnell, H. S. A. Ehrenreich, B. Assmus, and B. Schink.** 1993. Ferrous iron oxidation by anoxygenic phototrophic bacteria. Nature **362:** 834–835.
44. **Wu, J., and G. W. Luther III.** 1995. Complexation of Fe(III) by natural organic ligands in the Northwest Atlantic Ocean by a competitive ligand equilibrium method and a kinetic approach. Mar. Chem. **50:**159–178.
45. **Zadvorny, O. A., N. A. Zorin, and I. N. Gogotov.** 2006. Transformation of metals and metal ions by hydrogenases from phototrophic bacteria. Arch. Microbiol. **184:**279–285.